

30
6-12-85 W.B. ①

cat. #

DR-1070-7
I-21367

SLAC-PUB--3614
DE85 013067

REPRODUCED FROM
BEST AVAILABLE COPY

SLC INJECTOR MODELING*
H. HANERFELD, W. B. HERRMANNFELDT, M. B. JAMES, AND R. H. MILLER
Stanford Linear Accelerator Center
Stanford University, Stanford, California 94305

CONF-850504-123

Abstract

The injector for the Stanford Linear Collider is being studied using the fully electromagnetic particle-in-cell program MASK. The program takes account of cylindrically symmetrical RF fields from the external source, as well as fields produced by the beam and DC magnetic fields. It calculates the radial and longitudinal motion of electrons and plots their positions in various planes in phase space. Bunching parameters can be optimized and insights into the bunching process and emittance growth have been gained. The results of the simulations are compared to the experimental results.

Description and Specification of Collider Injector

The collider injector must provide two intense single RF bunches 50 ns apart with low emittance and reasonable spectrum. The design specifications for the collider injector are listed below:

Charge per bunch	12 nC = $7.5 \times 10^{10} e^-$ /bunch
Bunch length	$15^\circ \approx 15$ psec FWHM
Emittance	.03 π mgc - m
Energy	35 to 50 MeV

The collider injector (Fig. 1) consists of an electron gun, two 16th sub-harmonic bunchers, a 10 cm long S-band traveling wave buncher and a 3 m long S-band traveling wave accelerator. The sub-harmonic bunchers (SHB's) bunch the 2.5 nsec gun pulse by about a factor of 12, so that the bunch entering the S-band buncher is about 200 psec long. The S-band buncher compresses the bunch about a factor of 10, and raises its energy slightly to about 350 kV. There is no space between the buncher and the accelerator since space charge forces would cause the bunch to debunch rapidly in the absence of a compressing longitudinal electric field. A cut-off iris between the buncher and accelerator section permits independent adjustment of phase and RF power level for each.

Discussion of One-Dimensional Modeling Program

Electron bunching and capture in the injector was initially calculated using a computer simulation similar to that used by Mavrogenes *et al.*¹ We modeled the beam as 30 to 50 infinitely thin disks of charge with each disk divided into three concentric annular regions of equal charge. The program calculates the longitudinal position and energy of the annular regions as they move through the injector region. The force due to RF fields is modeled as a sinusoidal field at the fundamental frequency in each region. The space charge forces between annuli are found by solving for the average static force between annuli inside a smooth, grounded, conducting cylinder. Thus the program calculates the effects of space charge and image charges on the longitudinal motion of the electrons. The buncher and accelerator regions are immersed in a solenoidal magnetic field which provides radial focusing. Assuming that the solenoidal fields can keep the beam at a reasonably constant radius in each region, the radius of the annuli were chosen by estimating the Brillouin radius.

*Work supported by the Department of Energy, contract DE-AC03-76SF00515.

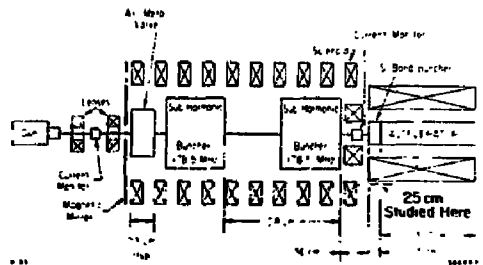


Fig. 1. The SLC Injector

This model should be satisfactory in the sub-harmonic buncher region where the conducting beam pipe is smooth. However, in the buncher and accelerator regions made up of disk-loaded waveguides, the model is a great over-simplification. Clearly, this one-dimensional program gives us no insight into transverse emittance growth which is a major (and undesirable!) by-product of the bunching process. Consequently, we decided to model the injector using the fully relativistic two-dimensional particle in cell program MASK.²

Buncher/Capture Region Modeled by MASK

The collider injector is about 6 m long, while the electron bunch is a few millimeters long. At present it is not reasonable to model the whole injector using MASK with the mesh size of about 1 mm required to represent the space charge forces of the final bunch wall. Consequently, we must seek piece-wise solutions. The most critical part of the injector is the S-band buncher and capture region of the accelerator where space charge forces and transverse emittance growth are largest. Thus the MASK runs reported here model a 25 cm long region beginning with the S-band buncher as indicated in Fig. 1. The emittance growth results from both space charge forces and the radial forces due to the RF fields. These effects vanish as $1/\gamma^2$.

Figure 2 is the R-Z profile of the buncher followed by the first three cavities of the S-band accelerator structure. The radius of the problem as simulated in MASK is smaller than the radius of the actual cavities. The upper boundary of each cavity is simulated as a "port" which has an RF voltage where phase and amplitude have been adjusted to simulate the traveling wave in the structure. This reduces the filling time required for the fields to reach steady state, since each cavity fills primarily from its own port.

These runs were made on the SLAC IBM 3081 and require only 10-20 minutes (depending on the number of macroparticles) for the actual simulation of the bunch passing through the structure. A somewhat longer time, about 40 minutes, is spent in carefully establishing the fields before the particles are injected, but this data is saved and then reused to restart the problem several times as different particle distributions, injection phase angles, etc., are simulated.

Poster paper presented at the 1985 Particle Accelerator Conference
Vancouver, B.C., Canada, May 13-16, 1985

DISTRIBUTION OF THIS DOCUMENT IS UNLIMITED

Results

Figure 2 represents particle density plots for a single bunch as it moves through the buncher and first three cavities of the accelerator. The bunch is shown at nine different times, not equally spaced, as it enters from the left, is bunched in the buncher and begins to be accelerated. It enters at 200 keV and leaves on the right at 1.5 MeV. Three different cases are shown in Fig. 2, all with the same initial RF fields before the bunch enters. The fields are 3 MV/m in the buncher and 17 MV/m in the accelerator. There is a uniform longitudinal DC magnetic field of .12 T applied in the first case. This field is the Brillouin field for the current of 100 A at the center of the bunch entering the problem. The first striking fact that we observe is that the volume the bunch occupies remains almost constant until it begins to be accelerated to relativistic velocities. In the first 1-7/8 RF cycle (first five photos) of Fig. 2a, the bunch length decreases by a factor 8 and the beam radius increases by about $\sqrt{8}$, thereby keeping the volume occupied by the beam almost constant.

In Fig. 2b we see what happens when we try to keep the beam smaller by increasing the focusing magnetic field. When we increase the field from .12 T to .15 T the beam does indeed stay smaller and the output emittance shrinks by 30% from $2.6 \times 10^{-4} \text{ } \mu\text{m}^2\text{-m}$ to $1.8 \times 10^{-4} \text{ } \mu\text{m}^2\text{-m}$. However, the bunch length increases from 21 ps to 27 ps.

We would like to point out another feature of the magnetic focusing. The ends of the bunch see lower radial space charge fields and hence are not at equilibrium. They oscillate about a smaller Brillouin radius (Figs. 2a and 2b). When the ends of the bunch are at large radius, the particles bunch more rapidly. This is because the longitudinal space charge forces decrease and the RF fields increase with increasing radius. The RF fields in the buncher increase with radius because $v_p < c$ and consequently the radial propagation constant k_r is imaginary. This effect is most striking in the third photo ($t = 1-1/8$ cycles) of Fig. 2b.

Figure 2c displays a run in which everything is identical to Fig. 2a except that the charge in the bunch has been reduced by a factor 100 to demonstrate the importance of the balance between the bunching forces and space charge. The electrons form a very short bunch in the third cell of the buncher, and then fly right through because the opposing space charge forces are too weak. A suitable reduction in RF field amplitude would cause a short bunch to form.

Figures 3 through 6 show different aspects of the computer run in Fig. 2a. They demonstrate the power of the MASK program to give insight into the beam dynamics in the injector.

Figure 3 shows the current distribution in the bunch as it passes five points almost equally spaced in z . The minimum full width at half maximum occurs in the cut off iris between the buncher and the accelerator. The FWHM increases somewhat after this point but the base of the bunch continues to bunch. The bunch shape does not change in the last 5 cm of the problem as the beam is being rapidly accelerated to relativistic velocities.

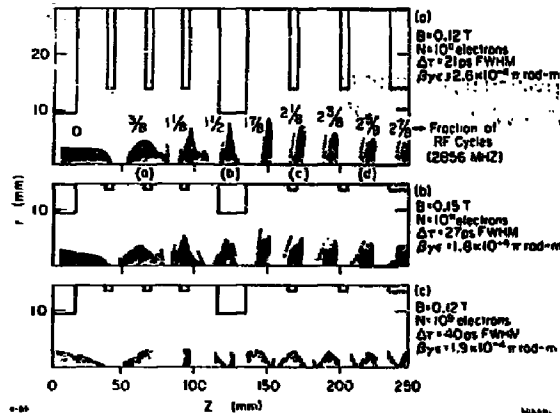


Fig. 2. The $R-Z$ particle density plots in each figure show the superimposed images of a single electron bunch. The electrons enter on the left from a subharmonic buncher, traverse the 0.75 velocity-of-light bunching section (the four cavities on the left) and are accelerated in the accelerating section (the first three cavities of which are simulated).

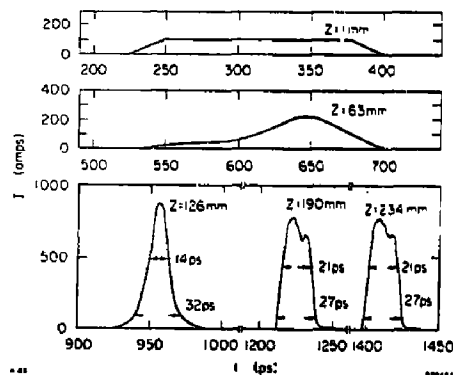


Fig. 3. The current distribution in the bunch for five values of z .

Figure 4 shows the longitudinal phase space of the beam of Fig. 2a as a function of z . At $z = a$ the beam displays the classical sinusoidal velocity modulation. By $z = b$, however, the space charge forces in the middle of the bunch are beginning to become stronger than the bunching fields and the correlation between momentum and s has reversed in a small region (see Fig. 4b). By $z = c$ (Fig. 4c) the bunch has a distinct positive correlation which means it is being debunched. However, by this point the energy is rising rapidly so very little debunching occurs. Due to the non-linear relationship between energy and velocity the particles which enter the buncher at both ends of the bunch are now behind the core, giving the beam a diffuse tail. By $z = d$ (Fig. 4d) a new feature has become apparent: the beam has a high frequency energy modulation with a

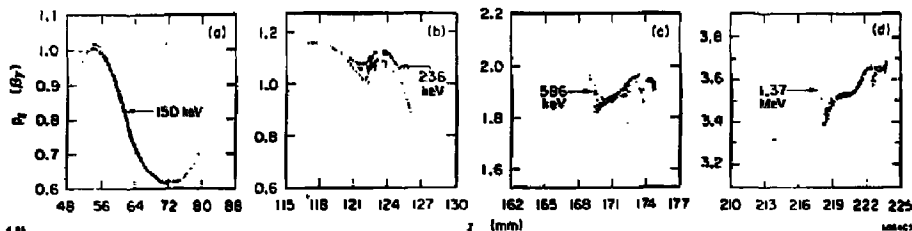


Fig. 4. Longitudinal phase space as a function of s for the beam shown in Fig. 2a.

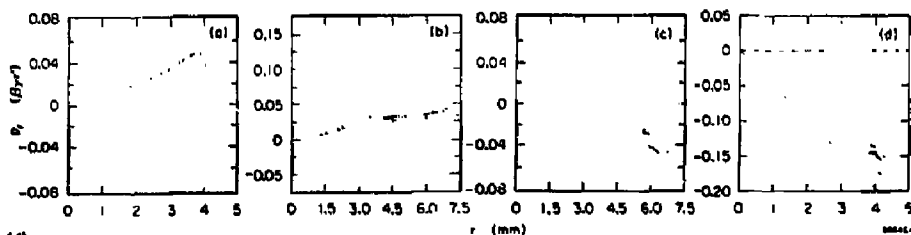


Fig. 5. Transverse phase space at same locations as shown in Fig. 4.

wavelength of 3 mm (i.e., about the 35th harmonic of the accelerator frequency). This may be real or it may be an artifact of the simulation.

The transverse phase space of the beam of Fig. 2a is shown in Fig. 5. Again, a, b, c, and d show the beam at $s = a, b, c,$ and $d,$ respectively. The most obvious feature of the radial phase space in Fig. 5a and b is that a diffuse halo is seen, populated by the particles from either end of the bunch which are mismatched into the Brillouin focusing solenoid. Another effect begins to appear in Fig. 5c and is obvious in 5d. The distribution of particles in the r, p_r phase plane becomes triangular. The spread in radial momentum p_r is a linear function of r . This results from the fact that the RF radial forces depend linearly on radius, but vary sinusoidally with time. This time-dependent RF lens dominates the output emittance of this injector.

The axial electric field, $E_z,$ is shown in Fig. 6. The injected bunch contains $1 \times 10^{11} e^-$ and the effect of the wakefields is apparent at the location of the bunch at about $s = 150$ mm. The 3 mm wave we mentioned earlier is also apparent behind the bunch.

Comparison with Experimental Results

We have not reached the point of doing a detailed comparison between the MASK calculations and experiments. The injector is now used for all full energy beams and is not available for tests. Measurements reported earlier³ indicate the emittance from the injector varies as $\beta\gamma\epsilon = 0.7 \times 10^{-4} \sqrt{I} \text{ rad} - \text{m},$ where I is the current in $10^{10} e^-/\text{pulse}.$ So for $10^{11} e^-$ we should expect $2.2 \times 10^{-4} \text{ rad} - \text{m}.$ The experimental bunch length reported in Ref. 3 was 16 ps FWHM for $5 \times 10^{10} e^-.$ The MASK runs gave bunch lengths of 21 to 27 psec for $10^{11} e^-$ and emittances of 1.8 to $2.6 \times 10^{-4} \text{ rad} - \text{m}.$

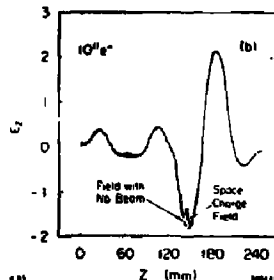


Fig. 6. Longitudinal electric field.

Conclusion

MASK is a powerful tool for designing and understanding high current electron linear accelerator injectors. The programs diagnostics allow the designer to see the bunch evolve, to watch the emittance grow, to see the effect of space-charge on the fields in the structure. Our next step will be to do careful comparisons with experimental data from the injector. In this process we hope to see whether the dependence on parameters such as magnetic field is the same as the MASK calculations indicate. Finally we hope to use MASK to design a bunching system which can bunch 2 or 3 times more charge into a single S-band bunch than our present injector.

References

1. G. Mavrogenes et al., IEEE Trans. Nucl. Sci. NS-20, 019, June 1973.
2. M. B. James et al., IEEE Trans. Nucl. Sci. NS-30, 2902, Aug. 1983.
3. A. Drobot, "Numerical Simulation of High Power Microwave Sources," this conference.

DISCLAIMER

This report was prepared as an account of work sponsored by an agency of the United States Government. Neither the United States Government nor any agency thereof, nor any of their employees, makes any warranty, express or implied, or assumes any legal liability or responsibility for the accuracy, completeness, or usefulness of any information, apparatus, product, or process disclosed, or represents that its use would not infringe privately owned rights. Reference herein to any specific commercial product, process, or service by trade name, trademark, manufacturer, or otherwise does not necessarily constitute or imply its endorsement, recommendation, or favoring by the United States Government or any agency thereof. The views and opinions of authors expressed herein do not necessarily state or reflect those of the United States Government or any agency thereof.